



PCCP

**Hydrogen-bonding in the pyrimidine...NH<sub>3</sub> van der Waals complex: Experiment and Theory**

Journal:	<i>Physical Chemistry Chemical Physics</i>
Manuscript ID:	CP-ART-04-2014-001472.R1
Article Type:	Paper
Date Submitted by the Author:	07-May-2014
Complete List of Authors:	Cockett, Martin; University of York, Department of Chemistry Gosling, Matthew; University of York, Department of Chemistry

SCHOLARONE™  
Manuscripts

## ARTICLE

# Hydrogen-bonding in the pyrimidine...NH<sub>3</sub> van der Waals complex: Experiment and Theory

Cite this: DOI: 10.1039/x0xx00000x

M. P. Gosling and M. C. R. Cockett<sup>a</sup>Received 00th January 2012,  
Accepted 00th January 2012

DOI: 10.1039/x0xx00000x

[www.rsc.org/](http://www.rsc.org/)

The pyrimidine...NH<sub>3</sub> van der Waals complex has been studied using a combination of resonant two-photon ionisation (R2PI) spectroscopy, *ab initio* molecular orbital calculations and multidimensional Franck-Condon analysis. The R2PI spectrum is assignable to a single stable conformer in which the ammonia molecule binds *via* two hydrogen bonds within the plane of the ring, in a location which minimises repulsion between the ammonia nitrogen lone pair and that of the second, more remote pyrimidine nitrogen in the 3 position on the opposite side of the ring. Ground state estimated CCSD(T) interaction energies were extrapolated to the complete basis set limit: these calculations found the dissociation energy of the most stable conformer,  $\sigma_B$ , to be 20% larger than that of a second in-plane conformer,  $\sigma_A$ , in which the ammonia forms a similar pseudo five-membered ring, bridging the nitrogen at the 1 position with the carbon at the 2 position. This conformation in turn was found to have a dissociation energy 35% larger than that of a  $\pi$ -complex in which the ammonia binds above the plane of the aromatic ring. The results of multidimensional Franck-Condon simulations based on *ab initio* ground and excited state CASSCF and RIC2 geometry optimisations and vibrational frequency calculations showed good agreement with experiment. It is postulated that longer-range electrostatic interactions between the ammonia lone pair and the more distant of the two ring nitrogens on the pyrimidine, play a key role in determining which of the two in-plane structures is the more stable and which, therefore, is responsible for all of the spectral features observed in the R2PI spectrum.

## 1 Introduction

Heteroaromatic molecules present interesting templates for hydrogen-bonding because they can act both as proton acceptors through the lone pairs on the heteroatoms and as proton donors. Heteroaromatic systems in which nitrogen atoms occupy positions within the aromatic ring are common in biological systems, most notably in DNA and RNA where recognition between bases is defined *via* linear amine (N-H...N) hydrogen bond formation at the nitrogen lone pairs. The structural motif conserved throughout all of the DNA and RNA bases is that of pyrimidine in which two nitrogen atoms occupy positions within the six-membered aromatic ring that are meta to one another. In addition to the familiar hydrogen bonding described above, cation- $\pi$  interactions between the aromatic rings of nucleic acid bases and positively charged amino acid side-chains have been shown to be quite common at the protein-DNA interface.<sup>1,2</sup> Given that heteroaromatic molecules are generally regarded as  $\pi$ -deficient, it is interesting to speculate to what extent the amino group in a polar but neutral amino acid might play a role in the inverse of a cation- $\pi$  interaction in which the nitrogen lone pair on the amino group

forms weak interactions with the electron-deficient  $\pi$ -system on a neighbouring base.

Model binary van der Waals complexes, studied in the gas phase using supersonic free jet expansion techniques, provide a means of establishing the intrinsic stabilities of different types of hydrogen bonding interaction, with the isolated environment of the complex allowing comparison with results from computational calculations. Under these conditions, the conformation lying lowest in energy on the free energy landscape will tend to dominate within the expansion and the solute and solvent will adopt orientations with respect to each other that are unperturbed by external factors that would hinder the conformational freedom in solution or in the biological context.

Whilst pyrimidine has been widely studied in various spectroscopic<sup>3,4,5,6,7,8</sup> and computational studies,<sup>9,10</sup> studies of binary complexes of pyrimidine are rather less numerous. Van der Waals complexes of pyrimidine with argon and nitrogen have been studied using ZEKE (Zero Electron Kinetic Energy) spectroscopy<sup>11</sup> whilst pyrimidine-water has been studied in the liquid phase using polarised Raman and in matrix isolation using FTIR (Fourier Transform Infra-Red) spectroscopy.<sup>12,13</sup>

These two latter studies used density functional theory (DFT) to determine that, in pyrimidine $\cdots$ H<sub>2</sub>O, one of the pyrimidine nitrogens plays the role of proton acceptor for one of the water hydrogens in a linear hydrogen-bonded structure. Thus far, however, pyrimidine $\cdots$ H<sub>2</sub>O has not been identified in the gas phase, in spite of a number of documented attempts, but has been the subject of computational study.<sup>14,15</sup>

The pyrimidine $\cdots$ NH<sub>3</sub> complex (Pyr $\cdots$ NH<sub>3</sub>) provides the simplest example of intermolecular association between an amine and a 1,3-diazabenzene. Bernstein and coworkers investigated this molecule as part of a broader study of a number of small molecular clusters in the gas phase using resonant two-photon ionisation (R2PI).<sup>16</sup> They identified three plausible structures for the complex using a rudimentary Leonard Jones potential. Two of the structures featured out-of-plane binding of the ammonia at the aromatic interface whilst the third featured a conventional in-plane hydrogen bond between the ammonia and one of the nitrogen lone pairs on the ring. The R2PI spectrum recorded in that study exhibited three more or less equally intense bands between +300 and +500 cm<sup>-1</sup> relative to the pyrimidine band origin. These three bands were assigned in that study as band origins associated with the three stable conformations of the complex. No intermolecular vibrational structure was observed in the spectrum and no inter- or intramolecular assignments made.

The first excited singlet state in pyrimidine is an  $n\pi^*$  state with a characteristically much smaller absorption cross section compared to the  $\pi\pi^*$  states that appear to higher energy. The resulting large difference in charge distribution between states means that any solvent molecules bound to the azabenzene experience a very different electronic environment in the excited state. This is likely to yield large spectral shifts associated with significant changes in binding strength which may then provide clear indication of the favoured ligand position.<sup>17</sup>

The aim of the present study is to re-examine the Pyr $\cdots$ NH<sub>3</sub> complex in much greater detail using two-colour R2PI spectroscopy combined with modern high level *ab initio* molecular orbital calculations. One of the key objectives will be to establish whether or not this complex does indeed exist in more than one stable conformation in the gas phase and in particular whether binding of the ammonia to the  $\pi$  system is competitive with hydrogen bonding to one of the ring nitrogens. The methods employed are identical to those used in recent studies of the fluorobenzene $\cdots$ NH<sub>3</sub> and 4-fluorotoluene $\cdots$ NH<sub>3</sub> complexes which combined R2PI spectroscopy with *ab initio* and Franck-Condon calculations.<sup>18,19</sup>

## 2. Experimental

The experimental setup is essentially that described in detail elsewhere.<sup>20</sup> Pyr $\cdots$ NH<sub>3</sub> was prepared in the gas phase using a supersonic free jet expansion of pyrimidine with ammonia and argon, at typical stagnation pressures of between 0.7 and 1 bar and at a typical sample reservoir temperature of 18°C.

Electronic excitation and ionisation was achieved using the Nd:YAG (Continuum Surelite III) pumped, frequency doubled output of one dye laser (Radiant Narrowscan using DCM) acting as pump, with the frequency doubled output of a second dye laser, (Continuum Jaguar using Coumarin 120 in methanol) acting as probe. The pump dye laser was calibrated using a neon optogalvanic lamp. All quoted energies are corrected to vacuum, but intensities of observed features have not been corrected to dye intensity profiles.

## 3. Computational

Molecular orbital calculations were performed using the GAUSSIAN 09 and TURBOMOLE 5.9 suites of programs.<sup>21,22</sup> Counterpoise corrected geometry optimisations and vibrational frequencies were initially performed on the electronic ground state of a number of different conformers of the neutral complexes using second order Møller-Plesset perturbation theory<sup>23</sup> with the cc-pVTZ correlation consistent basis set of Dunning. The choice of this basis set for the geometry optimisations derives from the results of Shibasaki *et al.* who found that the under-representation of the binding determined for  $\pi$ -complexes using the cc-pVTZ basis set compensates for the over-binding that results from the choice of the MP2 methodology.<sup>24</sup> As a result, the accuracy of MP2/cc-pVTZ level optimized geometries is generally very good and provides an excellent basis from which to perform higher level single point interaction energy calculations.

Interaction energies extrapolated to the complete basis set limit,  $\Delta E_{\text{MP2/CBS}}$ , were calculated at the MP2 level of theory using Helgaker's method to extrapolate from counterpoise corrected interaction energies obtained using pairs of adjacent quality basis sets.<sup>25</sup> In Helgaker's method, interaction energies calculated using Dunning's augmented correlation consistent basis sets are fitted to the form  $a+bX^{-3}$  (where  $X$  is 2 for aug-cc-pVDZ, 3 for aug-cc-pVTZ and 4 for aug-cc-pVQZ). The best results are obtained from extrapolations using aug-cc-pVTZ and aug-cc-pVQZ MP2 calculations. It is generally the case that MP2 over-stabilises dispersion bound  $\pi$ -complexes compared to in-plane hydrogen-bound complexes when employing larger basis sets.<sup>26</sup> The least expensive method of producing quantitatively accurate interaction energies for both hydrogen and dispersion bound complexes is the coupled cluster CCSD(T) method in which the single and double excitations are evaluated iteratively while triple excitations are included in a non-iterative way.<sup>27</sup> However, single point CCSD(T) calculations using large basis sets are hugely expensive for the size of system studied here and so the accepted approach involves applying a CCSD(T) correction to interaction energies computed at a lower level of theory. In the present case, this is achieved by performing counterpoise corrected single point CCSD(T) and MP2 calculations at the MP2/cc-pVTZ optimised geometry using the aug-cc-pVDZ basis set. The difference between CCSD(T) and MP2 interaction energies ( $\Delta E_{\text{CCSD(T)}} - \Delta E_{\text{MP2}}$ ) exhibits a relatively

small basis-set dependence compared to the MP2 and CCSD(T) energies and so an approximate CCSD(T) interaction energy extrapolated to the complete basis set limit,  $\Delta E_{\text{CCSD(T)/CBS}}$ , can be computed as a simple correction to  $\Delta E_{\text{MP2/CBS}}$ . This approach has been shown in a meticulous series of studies of a wide range of non-covalently bound systems to yield interaction energies with errors of less than  $0.1 \text{ kcal mol}^{-1}$ .<sup>28,29</sup>

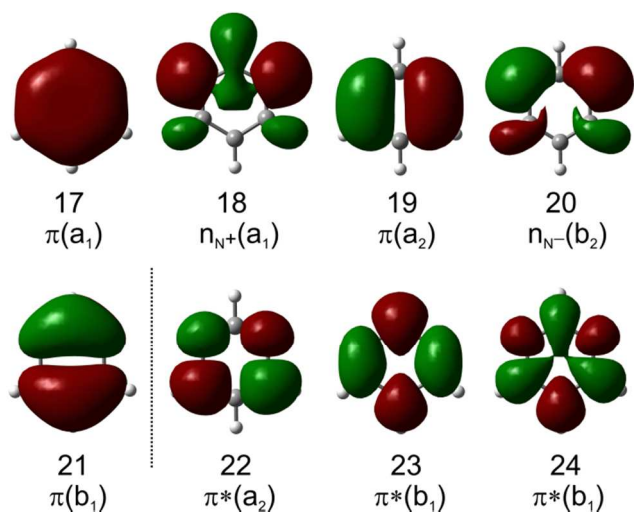


**Figure 1.** The CASSCF calculations used an active space with 10 electrons in six  $\pi$ -orbitals (three bonding and three anti-bonding) and two non-bonding orbitals,  $n_{\text{N}+}$  and  $n_{\text{N}-}$ . The vertical line in the figure shows the boundary between the HOMO and LUMO orbitals.

The change in geometry upon electronic excitation of different conformations of such weakly bound complexes provides one of the most important diagnostics in helping to identify which conformers are observed experimentally. Geometry optimisation and vibrational frequency calculations were performed on the electronic ground and first excited states of the most stable conformers of the neutral complexes using both RICC2<sup>30,31</sup> and CASSCF methods. Both ground and excited state CASSCF calculations used a (10,8) active space with ten electrons in six  $\pi$ -orbitals (3 bonding and 3 antibonding) and two non-bonding orbitals,  $n_{\text{N}+}$  and  $n_{\text{N}-}$  (see Figure 1). For the RICC2 calculations, the def2-TZVPP basis set of Ahlrichs<sup>32,33</sup> was used whilst the CASSCF calculations used both aug-cc-pVDZ and 6-311G(2f) basis sets, the latter equivalent in quality to the def2-TZVPP basis used in the RICC2 calculations. The results of these calculations were used to generate multidimensional Franck-Condon simulations for comparison with experiment (see reference 34 for further details of the method).

## 4. Results and Discussion

### 4.1. Experimental: The (1+1') R2PI spectrum of Pyr $\cdots$ NH<sub>3</sub>

The first  $800 \text{ cm}^{-1}$  of the (1+1') R2PI spectrum of Pyr $\cdots$ NH<sub>3</sub> is compared to that of pyrimidine in Figure 2. The spectra are presented in terms of relative internal energy to facilitate

comparison of intramolecular vibrational mode wavenumbers between the two species.

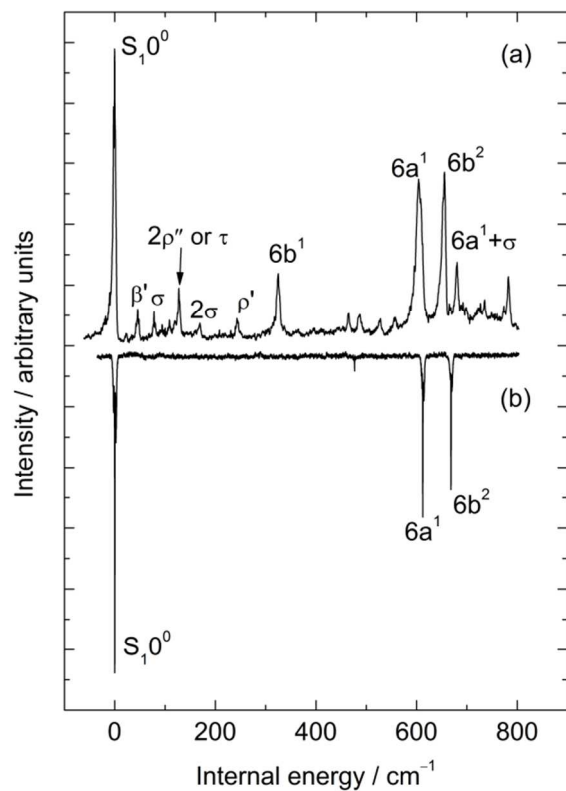


**Figure 2.** R2PI spectra of (a) Pyr $\cdots$ NH<sub>3</sub> and (b) pyrimidine presented in terms of internal energy relative to the respective  $S_1$  band origins.

The most intense band in the R2PI spectrum of pyrimidine, is assigned to the  $S_1$  band origin and appears at  $31081.0 \text{ cm}^{-1}$ , in good agreement with the values of  $31076 \text{ cm}^{-1}$  and  $31073 \text{ cm}^{-1}$  reported, respectively, by Riese and Grottemeyer<sup>6</sup> and by Sato *et al.*<sup>11</sup> Aside from the origin band, the only bands of significant intensity in this region are those at  $611.5 \text{ cm}^{-1}$  and  $668.5 \text{ cm}^{-1}$ , which are provisionally assigned here in line with earlier assignments to the  $6a^1$  ( $a_1$ ) fundamental and  $6b^2$  overtone ( $b_2 \times b_2$ ), appearing as a Fermi resonance.<sup>4,5,6</sup> It is worth noting at this point that these earlier assignments were made on the assumption that pyrimidine retains  $C_{2v}$  symmetry in its  $n\pi^*$   $S_1$  state; our own *ab initio* calculations suggest that it adopts an in-plane distorted structure, reducing its symmetry to  $C_s$  (see section 4.2.2(b)).

The R2PI spectrum of Pyr $\cdots$ NH<sub>3</sub>, recorded by gating on the Pyr $\cdots$ NH<sub>3</sub> mass channel, shows a strong band origin at  $31450.3 \text{ cm}^{-1}$  which appears  $369.3 \text{ cm}^{-1}$  to higher energy than that of pyrimidine. This substantial spectral blue shift indicates that the intermolecular interaction has weakened considerably in the  $S_1$  state compared to the electronic ground state. To higher energy the spectrum exhibits numerous vibrational bands of varying intensity which may reasonably be associated with intermolecular (van der Waals) or intramolecular modes, or

combinations between the two. Amongst these features, three bands stand out at 325.6, 604.1 and 655.7  $\text{cm}^{-1}$ , the latter two of which are straightforwardly assignable to the  $6a^1/6b^2$  Fermi resonance but displaying small but significant red shifts in comparison with the same band positions in pyrimidine. The band at 325.6  $\text{cm}^{-1}$  does not correlate obviously with any of the intramolecular bands in the pyrimidine spectrum but it is also rather high in wavenumber to be assigned to an intermolecular fundamental. However, it does sit half way between the origin band and the  $6b^2$  overtone which strongly suggests an assignment to the  $6b^1$  fundamental, appearing in the complex spectrum as a result of the lowering in symmetry of the complex compared with free pyrimidine. It is worth noting that all three bands are reported in Bernstein's paper although not displayed in the spectrum presented therein. Their assignments of the higher wavenumber bands are consistent with the literature assignments for pyrimidine,<sup>4</sup> with the lower wavenumber band assigned to  $6a^1$  and the higher to  $6b^2$ . No reference is made in that work to a band appearing at 326  $\text{cm}^{-1}$ .

The most notable difference between the pyrimidine spectrum and that of  $\text{Pyr}\cdots\text{NH}_3$  lies in the vibrational activity in the low wavenumber region below 250  $\text{cm}^{-1}$  internal energy for which no corresponding features appear in the pyrimidine spectrum. All of these features are most reasonably assignable to intermolecular modes of the complex. A complete spectral assignment of the R2PI spectra  $\text{Pyr}\cdots\text{NH}_3$  R2PI is shown in Table 1 together with those of pyrimidine. The assignments

given there are based predominantly on the Franck-Condon analysis discussed later on.

## 4.2. Ab initio calculations

### 4.2.1 Electronic ground State: geometries and interaction energies

Geometry optimisations conducted at the RIC2 level of theory and utilising the def2-TZVPP basis set identified three stable  $\text{Pyr}\cdots\text{NH}_3$  conformations in the  $S_0$  state (shown schematically in Figure 3). For two of the conformers (labelled  $\sigma_A$  and  $\sigma_B$ ), the ammonia binds in the plane of the ring whilst in the third (labelled  $\pi$ ), the ammonia sits above the plane of the ring, interacting with the aromatic  $\pi$ -system.

The  $\sigma_A$  and  $\sigma_B$  conformers both feature two hydrogen bonds and possess  $C_s$  symmetry with the aromatic plane defining a single plane of reflective symmetry. In each case a pyrimidine nitrogen lone pair acts as a proton acceptor for a single  $\delta^+$  ammonia hydrogen atom whilst the ammonia lone pair acts as a proton acceptor for a neighbouring  $\delta^+$  pyrimidine hydrogen. The result in each case is a cyclic hydrogen-bound system forming a pseudo five-membered ring. The  $\sigma_A$  and  $\sigma_B$  conformers differ in terms of which pyrimidine hydrogen is involved in the binding. In  $\sigma_A$  it is the hydrogen in the 2 ( $H_2$ ) position, bisecting the two nitrogen atoms, whilst in  $\sigma_B$  it is the hydrogen in the 6 ( $H_6$ ) position, on the opposite side of the ring to the second nitrogen,  $N_3$ . The main geometric difference between the two structures therefore, is the orientation and proximity of the ammonia with respect to the second pyrimidine nitrogen in the 3 position.

**Table 1.** Positions and assignments of vibrational bands in the R2PI spectrum of pyrimidine and  $\text{Pyr}\cdots\text{NH}_3$

Pyrimidine ( $S_1$ )			Pyrimidine $\cdots\text{NH}_3$ ( $S_1$ )		
One Photon Energy / $\text{cm}^{-1}$	$\Delta/\text{cm}^{-1}$	Assignment <sup>a</sup>	One Photon Energy / $\text{cm}^{-1}$	$\Delta/\text{cm}^{-1}$	Assignment <sup>a</sup>
31081.0	0	$S_10^0$	31450.3	0	$S_10^0$
			31495.0	44.7	$\beta'$
			31529.4	79.1	$\sigma$
			31578.5	128.2	$\tau$ or $2\rho''$
			31619.5	169.2	$2\sigma$
			31692.4	242.1	$\rho'$
			31775.9	325.6	$6b^1$
			31936.7	486.4	-
			31977.6	527.4	-
			32007.4	557.1	-
31692.5	611.5	$6a^1$	32054.4	604.1	$6a^1$
31749.5	668.5	$6b^2$	32105.9	655.7	$6b^2$
			32130.5	680.2	$6a^1 + \sigma$
			32183.0	732.7	$6b^2 + \sigma / 6a^1 + (\tau \text{ or } 2\rho'')$
			32232.4	782.1	$6b^2 + (\tau \text{ or } 2\rho'')$

<sup>a</sup> All assignments this work

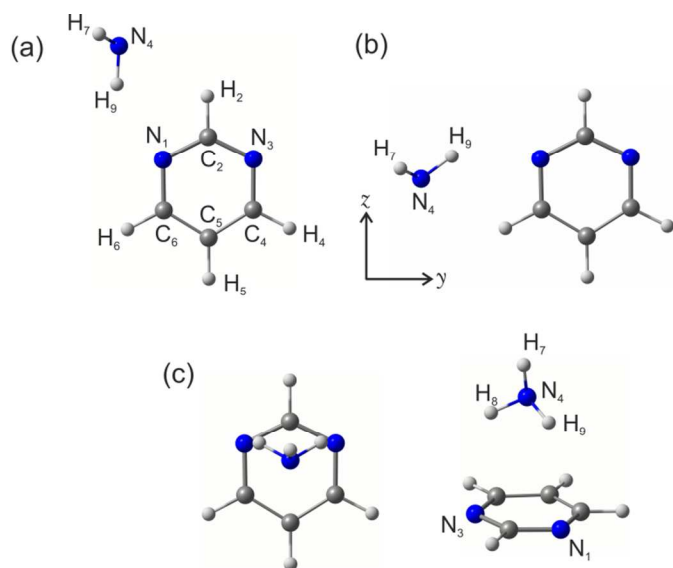


**Figure 3** Schematic diagrams of the three stable electronic ground state conformations of pyrimidine...NH<sub>3</sub>, (a)  $\sigma_A$  (b)  $\sigma_B$  and (c)  $\pi$ . Initial conformational searches performed at the RIC2/def2-TZVPP level of theory.

The  $\pi$  structure is also of  $C_s$  symmetry but in this case the plane of reflective symmetry is oriented perpendicular to the pyrimidine plane. In this conformation, the ammonia sits with two of its three hydrogen atoms directed towards the two pyrimidine nitrogens with the ammonia nitrogen atom sitting more or less centrally at a distance 3.192 Å above the centre of the aromatic ring. The ammonia is inclined in such a way that the ammonia nitrogen lone pair points along an axis essentially parallel with the plane of the ring: the impression given then is one of a balance between two points of hydrogen-bond interaction between the ammonia hydrogens and the ring nitrogen lone pairs, whilst the ammonia lone pair sits in a somewhat neutral attitude above the  $\pi$ -system of the aromatic ring, inclined towards the C<sub>5</sub> carbon. Although this conformation is one in which the ammonia sits above the ring, it is not one which might reasonably be described as a  $\pi$ -hydrogen bond. The stability of this structure almost certainly owes something to the influence of the electronegative nitrogen atoms of pyrimidine which result in an electron-deficient aromatic system which is able to gain stability by accepting partial charge from the ammonia lone pair. Rather than forming an aromatic hydrogen bond therefore (as are prevalent in out-of-plane complexes with electron rich  $\pi$ -systems), the role of the aromatic interface is reversed and it acts as a lone-pair acceptor.

Counterpoise corrected interaction energies extrapolated to the complete basis set limit were computed for all three conformers of Pyr-NH<sub>3</sub> at the MP2 and CCSD(T) levels of theory using the approach described in the computational section above. Table 2 shows the results of extrapolations obtained from the MP2/aug-cc-pVTZ and MP2/aug-cc-pVQZ energies. In addition, the computed differences in MP2/cc-pVTZ zero point energies between complexes and fragments,

$\Delta ZPE$ , allowed dissociation energies (essentially zero point interaction energies),  $D_0$ , to be calculated in each case.

The results of these calculations are interesting: the most stable of the three conformers is the  $\sigma_B$ -complex whose calculated dissociation energy is about 20% larger than that of the closely related  $\sigma_A$ -complex which, in turn, is about 35% larger than the  $\pi$ -complex. This result would appear to be inconsistent with the reported observation of three stable conformers in the earlier work of Bernstein and coworkers.<sup>16</sup> Their force field calculations suggested the most stable conformation to be a  $\pi$ -conformation (structure I in that work) in which the ammonia straddles the ring with all three hydrogens pointing downwards, closely followed by a second  $\pi$ -conformation (structure II) which resembles somewhat the  $\pi$ -complex found from the *ab initio* calculations conducted as part of the present work.

The results of the calculations presented here instead support the conclusion that pyrimidine...NH<sub>3</sub> exists predominantly in a single conformation in the gas phase with all of the spectral features observed in the R2PI spectrum then attributable to that single structure. In particular, the influence of the two electronegative nitrogen atoms in pyrimidine clearly undermines the viability of a  $\pi$ -complex when competing with the much more stable prospect of one of two double-hydrogen bonded in-plane  $\sigma$ -complexes.

**Table 2** Counterpoise corrected MP2 and CCSD(T) interaction energies in cm<sup>-1</sup> for the two most stable conformers of the Pyr...NH<sub>3</sub> complex.

	Pyr...NH <sub>3</sub> / cm <sup>-1</sup>		
	$\sigma_A$	$\sigma_B$	$\pi$
MP2/aug-cc-pVDZ	1137.7	1363.4	838.4
MP2/aug-cc-pVTZ	1245.7	1481.5	925.3
MP2/aug-cc-pVQZ	1284.4	1523.9	954.6
MP2/CBS	1312.6	1554.8	976.0
CCSD(T)/aug-cc-pVDZ	1125.7	1338.7	721.4
CCSD(T)-MP2/aug-cc-pVDZ	-12.0	-25.0	-117.0
CCSD(T)/CBS	1300.6	1529.8	859.0
$\Delta ZPE^b$	-418.5	-453.9	-245.6
$D_0(\text{calc})$	882.1	1075.9	613.4

<sup>a</sup> Computed at the counterpoise corrected MP2/cc-pVTZ optimised geometry.

<sup>b</sup> MP2/cc-pVTZ

The two in-plane structures both involve double hydrogen bonds and, were it not for the presence of the second ring nitrogen in pyrimidine, would be energetically equivalent. However, the *ab initio* calculations show quite clearly that the preferred conformation is one in which the ammonia lone-pair forms a hydrogen bond to the ring hydrogen at the 6 position, on the opposite side of the ring to the second nitrogen at the 3 position. The stability of this structure over that where the ammonia bridges the N<sub>1</sub> nitrogen and the carbon at the 2 position (C<sub>2</sub>), can be rationalised in terms of the long-range electrostatic interaction between the ammonia lone pair and that of the more distant ring nitrogen: In the case of the  $\sigma_A$  complex, the ammonia lone pair has a direct line of sight to the potential presented by the lone pair of the nitrogen at the 3 position whereas for the  $\sigma_B$  complex, the same nitrogen is

effectively obscured from view. Consequently, for  $\sigma_A$  the additional repulsive interaction destabilises this conformer relative to  $\sigma_B$  to the extent that the former is evidently not observed in the spectrum.

#### 4.2.2 The $S_1$ state: spectral shifts, geometry changes and vibrational frequencies

##### (a) Spectral shifts

The three optimised ground state structures were each used as starting points in ( $n\pi^*$ ) excited state geometry optimisations and vibrational frequency calculations using the RICC2/def2-TZVPP and CASSCF(10,8)/6-311G(2df) levels of theory. All optimisations were unconstrained and run at  $C_1$  symmetry to allow the greatest degree of freedom in locating viable minima. For the RICC2 calculations, stable excited state minima were found for all three conformers but the  $\pi$ -complex was found to have converged to a  $\pi^*(b_1) \leftarrow n_N-(b_2)$  state for which the ring distorted to a puckered, non-planar structure. The CASSCF calculations failed to locate a  $\pi$ -complex minimum for the  $\pi^*(a_2) \leftarrow n_N-(b_2)$  state, converging instead to the  $\sigma_A$  structure. For both methods, the  $\sigma_A$  complex was found to be the most stabilised by electronic excitation whilst the  $\sigma_B$  conformer is the most destabilised. From the RICC2 calculations, the  $\pi$ -complex showed only a moderate destabilisation upon electronic excitation but as this corresponds to a different  $n\pi^*$  electronic state the computed shift is only of incidental interest.

The very different behaviour of the two  $\sigma$ -complexes is surprising but can be understood by considering the  $n\pi^*$  nature of the excitation. The  $\pi^* \leftarrow n$  electronic excitation reduces the electron density in the pyrimidine lone-pair orbitals which, in the case of the  $\sigma_B$  conformer, weakens the intermolecular interaction and gives rise to a large predicted spectral blue shift (+168.4  $\text{cm}^{-1}$  for RICC2/def2-TZVPP and +236.3  $\text{cm}^{-1}$  for CASSCF/6-311G(2df)) with the CASSCF calculation yielding a shift closest in magnitude to the experimentally observed value of +369  $\text{cm}^{-1}$  (see Table 3). However, the same excitation in the  $\sigma_A$  conformer results in a substantial stabilisation of the interaction and a large predicted spectral red shift (-293.6  $\text{cm}^{-1}$  for RICC2/def2-TZVPP and -191.4  $\text{cm}^{-1}$  for CASSCF/6-311G(2df)). This stabilisation in binding for  $\sigma_A$  can be rationalised by considering that the  $n\pi^*$  excitation arises from an orbital that spans both pyrimidine lone pair sites and so the reduction in lone pair electron density upon excitation will also be distributed between the two ring nitrogen lone pair orbitals. This means that although the nitrogen adjacent to the ammonia becomes less attractive for hydrogen bond formation, the unbound nitrogen also exerts a much smaller repulsive influence on the ammonia lone pair and it is this change in electronic environment which seemingly carries the greater weight in determining the net strength of the interaction. The change in interaction in the  $\sigma_A$  conformer is defined therefore by the component of the interaction that is most affected by the excitation, whether that be the stabilisation obtained by the decrease in the cross repulsion or the destabilisation caused by the weakening of the hydrogen bond. Intuitively, one might

reasonably expect the closer-range hydrogen bond to exert a greater influence over the net strength of interaction than the long range cross repulsion if the excitation resulted in an evenly distributed loss of electron density across the two pyrimidine nitrogen lone pairs. However, the large calculated red-shift suggests that the excitation gives rise to a state in which the electron density is distributed unevenly between the two nitrogen atoms in the excited state with a greater loss in density occurring at the more distant nitrogen than the one immediately adjacent to the ammonia. The calculated  $S_1 0^0$  band origins and spectral shifts for all three conformers of  $\text{Pyr} \cdots \text{NH}_3$  relative to pyrimidine are shown in Table 3.

Given the clear differences in predicted stability changes between the two most stable conformers, the large observed spectral blue shift of +369  $\text{cm}^{-1}$  in the experimental R2PI spectrum would appear to best support an assignment of the spectrum to the  $\sigma_B$ -complex. The larger magnitude of the experimental blue shift compared to the largest prediction (+276.0  $\text{cm}^{-1}$ ) suggests that the imbalance in the excitation between the two ring nitrogens is underestimated by the calculations. The large predicted red-shift for  $\sigma_A$  prompted a thorough search for bands in the R2PI to the red of the pyrimidine  $S_1$  band origin. However, a scan as far as 1000  $\text{cm}^{-1}$  to lower energy revealed no sign at all of any features which might be attributable to this conformer and so we conclude therefore that  $\text{Pyr} \cdots \text{NH}_3$  forms just a single stable conformation in the gas phase. Consequently, most of the remaining discussion presented here will focus solely on the  $\sigma_B$  conformer.

**Table 3.** Calculated  $S_1 0^0$  band origins and spectral shifts for the three most stable conformers of the  $\text{Pyr} \cdots \text{NH}_3$  complex relative to Pyr.

Species	RICC2/def2-TZVPP		CASSCF/6-311G(2df)	
	$S_1 0^0 / \text{cm}^{-1}$	$\Delta / \text{cm}^{-1}$	$S_1 0^0 / \text{cm}^{-1}$	$\Delta / \text{cm}^{-1}$
Pyr	30590.1	-	34098.1	-
$\sigma_A$	30296.5	-293.6	33906.7	-191.4
$\sigma_B$	30758.5	+168.4	34334.4	+236.3
$\pi$	30623.1 <sup>§</sup>	+32.9 <sup>§</sup>	-	-

<sup>§</sup> The only stable RICC2 excited state structure for the  $\pi$ -complex converged to the  $\pi^*(b_1) \leftarrow n_N-(b_2)$  state rather than the  $\pi^*(a_2) \leftarrow n_N-(b_2)$   $S_1$  state.

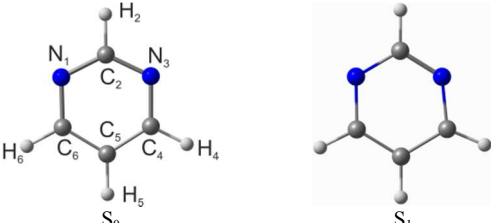
##### (b) Intramolecular geometry changes

The changes in intermolecular geometry that accompany electronic excitation are primarily driven by the effects of the redistribution of electron density that occurs in pyrimidine upon electronic excitation but this electronic change also determines the extent to which the pyrimidine geometry itself changes between the two electronic states. Table 4 shows selected geometric parameters derived from RICC2/def2-TZVPP and CASSCF/6-311G(2df) ground and excited state calculations for pyrimidine. In its electronic ground state, pyrimidine adopts a  $C_{2v}$  structure with the aromatic plane defining one of the planes of symmetry and the other, a perpendicular plane bisecting the opposing nitrogens along the axis containing the carbons at the 2 and 5 positions. Thus in its ground state the two heteroatoms are geometrically equivalent. However, upon electronic

excitation, although the molecule remains planar, the perpendicular plane of symmetry is lost and the overall symmetry reduces to  $C_s$ . This loss of symmetry is exemplified in the changes in internal bond angles which define the relationship between the two nitrogens and their neighbouring carbons, and in the distances between the two nitrogens and between the  $C_2$  and  $C_5$  carbons. Electronic excitation predominantly involves a transition from the HOMO-1 N-N anti-phase  $n_{N^-}(b_2)$  orbital into the LUMO  $\pi^*(a_2)$  antibonding orbital (see Figure 1), whose character is predominantly antibonding along the two longitudinal N-C bonds. This naturally results in the molecule lengthening along the  $C_2C_5$  axis which correlates with predicted activity in the 6a normal mode coordinate upon electronic excitation. However, the excitation also results in one of the two nitrogen atoms moving inwards towards the longitudinal axis, breaking the symmetry of the ring. The predicted response in other respects of the ring to this change depends on the computational method used: although both methods show that the  $C_2N_3C_4$  bond angle opens significantly more than the opposing  $C_2N_1C_6$  angle as the nitrogen moves inboard, the RICCF calculations suggest that this change accompanies a significant reduction in the  $C_2N_3$  bond length whereas the CASSCF calculations suggest that this bond remains essentially unchanged, with the opposing  $N_1C_2$  bond reducing in length. These differences, and others, are significant enough that they are likely to lead to differences in the predicted activity of particular normal modes upon electronic excitation, something which should become apparent in the Franck-Condon calculations discussed later. However, a reasonable expectation of multi-reference methods such as CASSCF is that they ought to provide a better description of the multi-configurational nature of an electronically excited state and consequently, a more accurate geometry than a single reference method such as CC2. The competing strength of CC2 is that it provides much more accurate excitation energies (see Table 3).

Such  $n\pi^*$  ring distortions in azabenzenes are not unprecedented: pyridine has been found to adopt a distorted boat structure in its  $n\pi^*$   $S_1$  state<sup>35</sup> whilst a  $C_s$  distorted structure has been proposed for the  $n\pi^*$  state in pyridazine.<sup>36</sup> It is not unreasonable therefore to postulate that pyrimidine responds in a similar way but to do so requires a consideration of whether the two nitrogen lone pair orbitals can be regarded as localised or delocalised. If the latter, then one might reasonably expect excitations involving the out-of-phase  $n_{N^-}$  or in-phase  $n_{N^+}$  orbitals to result in geometry changes that reflect the extent of that delocalisation. If the former, then the changes in electron density might be expected to occur predominantly on one side of the ring rather than the other, leading to a lowering of symmetry about the vertical reflective plane. However, it is also the case that an  $\pi^* \leftarrow n$  transition is one which results in seven  $\pi$ -electrons rather than the six required for Hückel aromaticity. The resulting anti-aromaticity may then prevent the ring from maintaining a regular symmetric structure, resulting in distortions of the type described above.

**Table 4.** A selection of geometric parameters for the  $S_0$  and  $S_1$  states of pyrimidine computed at the RICCF2/def2-TZVPP and CASSCF(10,8)/6-311G(2df) levels of theory. Bond lengths are given in angstroms and bond angles in degrees



	RICCF2	CASSCF	RICCF2( $\Delta$ )	CASSCF ( $\Delta$ )
$N_1C_2$	1.338	1.325	1.351 (+0.013)	1.295 (-0.030)
$C_2N_3$	1.338	1.325	1.300 (-0.038)	1.321 (-0.004)
$N_1C_6$	1.340	1.326	1.391 (+0.051)	1.404 (+0.078)
$N_3C_4$	1.340	1.326	1.385 (+0.045)	1.387 (+0.061)
$C_4C_5$	1.389	1.386	1.416 (+0.027)	1.387 (+0.001)
$C_6C_5$	1.389	1.386	1.370 (-0.019)	1.382 (-0.004)
$C_2C_5$	2.659	2.649	2.788 (+0.129)	2.767 (+0.118)
$N_1N_3$	2.402	2.368	2.271 (-0.131)	2.250 (-0.118)
$N_1C_2N_3$	127.6	126.6	117.8 (-9.8)	118.6 (-8.0)
$C_6C_5C_4$	116.8	116.6	117.8 (+1.0)	118.6 (+2.0)
$N_1C_6C_5$	122.4	121.9	122.2 (-0.2)	121.3 (-0.6)
$C_2N_3C_4$	115.4	116.5	127.4 (+12.0)	127.0 (+10.5)
$C_2N_1C_6$	115.4	116.5	119.5(+4.1)	119.8(+3.3)
$N_1C_2H_2$	116.2	116.7	120.6(+4.4)	121.6(+4.9)
$N_3C_2H_2$	116.2	116.7	121.6(+5.4)	119.8(+3.1)

A working hypothesis then is that the distortion of the ring, deriving from the compromised aromaticity, results in uneven bond angles about the two ring nitrogens with the electron density then favouring the nitrogen with the smaller bond angle to minimise valence shell electron pair repulsion. In both  $\sigma_A$  and  $\sigma_B$  conformers, the ammonia binds to the side of the ring with the smaller CNC bond angle and hence larger implied nitrogen lone-pair electron density in the excited state. For the  $\sigma_B$  conformer, whose binding is defined largely through the double hydrogen bond involving the  $N_1$  nitrogen and the  $H_6$  hydrogen of pyrimidine, electronic excitation will necessarily weaken the interaction as the lone-pair electron density reduces. However, as discussed above, the change in the strength of the interaction in the  $\sigma_A$  conformer will be dominated by the component of the interaction that is most affected by the excitation, whether that be the destabilisation resulting from the weakening lone pair electron density on the closest nitrogen or the decrease in the cross repulsion provided by the more distant of the two ring nitrogens. If the electron density on that nitrogen is disproportionately reduced compared to that on the more proximate nitrogen then we might expect a larger net contribution from the stabilisation resulting from the decrease in cross-repulsion than from the destabilisation resulting from the reduction in electron density on the  $N_1$  nitrogen. The net result of all of this is a spectral red-shift for the  $\sigma_A$  complex and a spectral blue-shift for the  $\sigma_B$  complex.

Whether a distorted structure in pyrimidine represents a stable minimum deep enough to accommodate the zero point level or sits within a weak minimum in a pseudo-symmetric



structure is a question which we plan to address in more detail in future work. What is clear though is that solvating the molecule, regardless of where the solvent binds, will lower the overall symmetry and will provide an additional incentive for the ring to distort. For both of the  $\sigma_A$  and  $\sigma_B$  complexes, the formation of in-plane hydrogen bonds between the ammonia and just one of the two pyrimidine nitrogen lone pairs means that some distortion of the ring might be expected even in the ground state, and indeed such distortions are observed although to a rather minor extent. For the  $\pi$ -complex, one might expect less of an inclination for the ring to deviate from a  $C_{2v}$  structure in the ground state and this expectation too is fulfilled. However, in the excited state, while the changes in key intramolecular parameters between the two states do differ slightly from one conformer to another, the underlying changes are essentially the same as in free pyrimidine which suggests that as far as intramolecular changes are concerned, the natural inclination of pyrimidine dominates, with the ammonia providing a relatively minor perturbation. Of greater significance in arriving at a confident assignment of a particular structure to the observed spectrum is the change in intermolecular parameters describing how the ammonia changes its orientation with respect to the pyrimidine upon electronic excitation.

### (c) Intermolecular geometry changes

The overall change in orientation of the ammonia with respect to the pyrimidine ring in the  $\sigma_B$ -conformer (see Figure 4) is relatively modest, characterised by a very small contraction in the hydrogen bond between the ammonia hydrogen ( $H_9$ ) and the adjacent pyrimidine nitrogen ( $N_1$ ) upon electronic excitation, and a larger increase in the second hydrogen bond length,  $N_4H_6$  by 0.147 Å. The overall increase in distance between the ammonia centre-of-mass and that of the pyrimidine is consistent with a predicted blue-shift and an overall weakening in the intermolecular interaction. The rather static position of the in-plane ammonia hydrogen though is somewhat at odds with the expectation that electron density will have reduced on the neighbouring pyrimidine nitrogen but it may be that the biasing of excited state lone pair density on the side of the ring with the smaller internal CNC bond angle partially compensates for the loss of an electron from the  $n_{N-}$  orbital. The increase in the  $N_4H_6$  bond length on the other hand suggests that the  $H_6$  ring hydrogen is rather less acidic in the excited state than in the ground state. The overall weakening, in particular, of this hydrogen bond results in the  $N_4H_9N_1$  bond angle opening up quite significantly (from 139.5° to 146.9°) as the ammonia tilts back away from the ring. These changes all occur within the plane of the molecule and suggest that electronic excitation will excite vibrational activity in the  $yz$  intermolecular bend or rock modes as well as a measure of the intermolecular stretching mode.

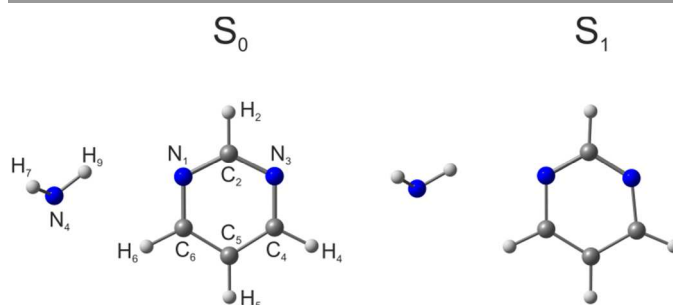


**Figure 4.** Optimised geometries of the  $\sigma_B$  conformer of Pyr...NH<sub>3</sub> in the  $S_0$  ground state (left) and  $S_1$  excited state (right) computed at the CASSCF/6-311G(2df) level of theory.

It is worth noting that a change in basis set to aug-cc-pVDZ results in a minimum for the  $\sigma_B$  conformer in which the ammonia rotates very slightly out-of-plane (about 1°): the additional diffuse functions associated with the  $\pi$ -system may in this case be providing an additional incentive to draw one of the ammonia hydrogens slightly out of the plane, and then slightly lowering the symmetry compared with the structures obtained with the 6-311G(2df) basis. A selection of computed  $S_0$  and  $S_1$  state geometric parameters for the  $\sigma_B$  conformer is given in Table 5.

**Table 5.** A selection of geometric parameters calculated at the CASSCF/6-311G(2df) level of theory for the neutral ground ( $S_0$ ) and first electronically excited ( $S_1$ ) states of the  $\sigma_B$ -conformer of Pyr...NH<sub>3</sub>. Bond lengths and intermolecular distances are given in Ångströms and bond angles in degrees. See Figure 4 for atom numbering.

Parameter	$S_0$	$\sigma_B$		$\Delta$
		$S_1$		
$N_4H_6$	2.557	2.535		-0.022
$H_9N_1$	2.731	2.876		+0.145
$N_4H_9N_1$	139.5	146.9		+7.4
$N_4H_6C_6$	124.5	122.6		-1.9

### 4.2.3 Excited State Vibrational Frequency Analysis and Franck-Condon Simulations

Harmonic vibrational frequencies were calculated at the CASSCF level of theory for the ground and first excited states of the  $\sigma_B$ -conformer using both 6-311G(2df) and aug-cc-pVDZ basis sets (as well as at the RICC2/def2-TZVPP for the purposes of comparison). The associated vibrational modes for the complex can be categorised as either intermolecular, which describe motion of the ammonia against the pyrimidine chromophore, or intramolecular which map onto the normal modes of pyrimidine or ammonia. Schematic representations of the six van der Waals normal mode vibrations plus two key intramolecular modes are shown in Figure 5 whilst a selection of computed  $S_1$  vibrational wavenumbers up to 1000  $\text{cm}^{-1}$  are given in Table 6.

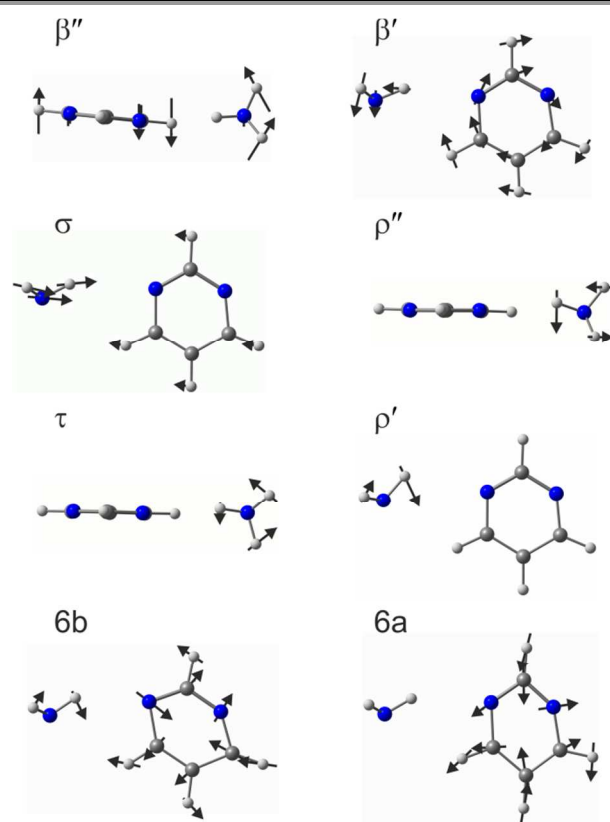


Figure 5. Schematic representations of the six van der Waals normal mode vibrations plus 6b and 6a intramolecular modes for the  $\sigma_B$  conformer of Pyr...NH<sub>3</sub>.

The eight lowest calculated  $S_1$  state wavenumbers using the 6-311G(2df) basis set are 31.9, 51.2, 86.5, 101.1, 146.2, 239.8, 294.0 and 319.5  $\text{cm}^{-1}$ . Six of these are intermolecular modes and two intramolecular. The first five can be characterised, respectively, as fundamentals in the ammonia out-of-plane bend,  $\beta''$ , the in-plane bend  $\beta'$ , the van der Waals stretch,  $\sigma$ , the out-of-plane rock,  $\rho''$  and the NH<sub>3</sub> internal rotation,  $\tau$ . The wavenumbers at 239.8 and 319.5 are the Pyr 16a and 11 mode fundamentals, best described as a ring twist about the axis bisecting the carbons at the 2 and 5 positions, and the ring flap along the same axis, respectively. The last of the six intermolecular fundamentals at 294.0  $\text{cm}^{-1}$ , is the in-plane rock,  $\rho'$ . A change to the aug-cc-pVDZ basis set results in quite substantial changes to all of the intermolecular modes, reflecting a softening in the potential with this basis, with the most dramatic change being to the out-of-plane modes,  $\beta''$  and  $\rho''$ .

The changes in geometry that accompany electronic excitation correlate directly to vibrational activity in the absorption spectrum *via* the Franck-Condon factors (at least to first order). Correspondingly, a measure of the extent to which the proposed conformation is consistent with the experimental R2PI spectrum can be obtained by performing a Franck-Condon analysis. The approach taken here uses the coherent state model of Doktorov *et al.*<sup>37</sup> with any differences in the

standard orientation of the two states being accounted for by the inclusion of a Hougen-Watson axis switching matrix into the standard linear Duschinsky normal coordinate transformation procedure.<sup>38,39</sup> The geometries and frequencies used in the simulations were those obtained from the ground and excited state RIC2/def2-TZVPP and CASSCF calculations, the latter employing both 6-311G(2df) and aug-cc-pVDZ basis sets.

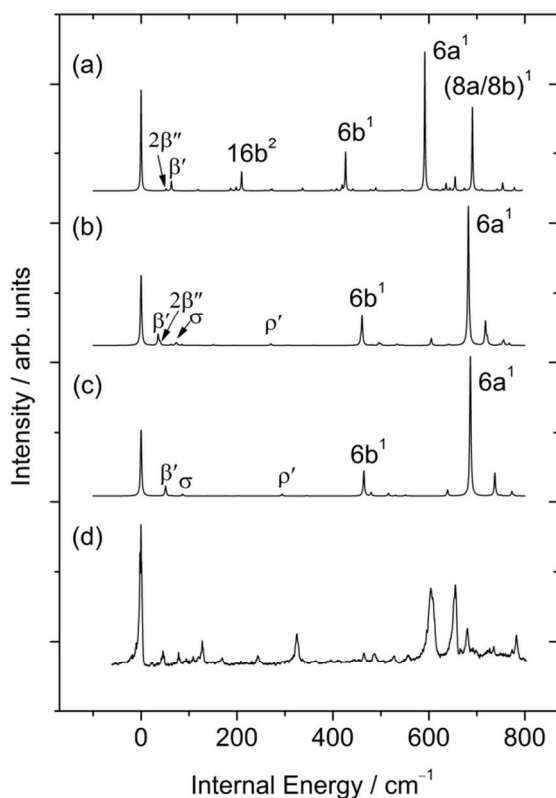
The Franck-Condon simulations<sup>40</sup> generated from the raw *ab initio* optimised structures and frequencies for the  $\sigma_B$ -conformer are compared with the experimental R2PI spectrum in Figure 6. All of the spectra show weak intermolecular vibrational activity, predominantly in the in-plane bend,  $\beta'$ , and van der Waals stretch,  $\sigma$ , with one or two simulations also predicting intensity in the first overtone in the out-of-plane bend  $\beta''$ .

Table 6. Computed  $S_1$  state CASSCF vibrational wavenumbers for the  $\sigma_B$ -conformer of the Pyr...NH<sub>3</sub> complex.

6-311G(2df) / $\text{cm}^{-1}$	$\sigma_B$ aug-cc-pVDZ / $\text{cm}^{-1}$	Assignment
31.9	19.7	$\beta''$
51.2	35.6	$\beta'$
86.5	73.7	$\sigma$
101.1	42.6	$\rho''$
146.2	131.4	$\tau$
239.8	228.9	16a
294.0	270.1	$\rho'$
319.5	302.5	11
457.2	444.4	16b
464.4	460.6	6b
570.2	552.1	-
686.4	682.3	6a
697.4	670.5	-
945.5	921.3	-
947.2	953.0	14/8b
975.9	954.6	-
982.4	983.5	18b

Regardless of the method or basis set used, all of the simulated spectra show a strong band origin together with strong activity in the 6a mode, in line with the predicted lengthening in the lateral C-C bond lengths for all conformations. All simulations predict stronger intensity in this band than appears in the experimental spectrum which suggests that the calculations over-estimate the change in this normal coordinate compared to what happens in reality. In addition to 6a, all simulations show weaker but significant activity in the 6b mode. This latter band appears because the calculations all predict an in-plane distortion to the ring in which one of the nitrogen atoms moves in-board upon electronic excitation, a geometry change which is best described as a diagonal ring distortion correlating most obviously with the 6b mode. The intensity of this band bears comparison with that of a conspicuous band appearing at about 325  $\text{cm}^{-1}$  in the experimental spectrum, which itself lies about half-way to the band at about 656  $\text{cm}^{-1}$  which has been assigned elsewhere to the 6b<sup>2</sup> overtone. A reasonable assignment here then would be to assign the 325  $\text{cm}^{-1}$  band to the 6b fundamental which appears in the Pyr...NH<sub>3</sub> complex spectrum with an

intensity which reflects both of the extent of the in-plane ring distortion but also the fact that in the complex the overall symmetry of the molecule is lowered much more emphatically compared with bare pyrimidine: this lowering of symmetry then relaxes further the selection rules permitting observation of single quanta excitation in modes which break the  $C_{2v}$  symmetry of ground state pyrimidine.



**Figure 6.** A comparison of multidimensional Franck-Condon simulations for the  $\sigma_B$ -conformer of Pyr...NH<sub>3</sub> at (a) RICC2/def2-TZVPP, (b) CASSCF/aug-cc-pVDZ and (c) CASSCF/6-311G(2df) levels of theory with (d) the experimental R2PI spectrum. All simulations based on the raw *ab initio* geometries and frequencies.

Where all of the CASSCF calculations share the same overall pattern of weak intermolecular activity combined with activity in the 6b and 6a ring modes, the RICC2 calculations show additional complexity deriving from overtones in out-of-plane ring modes as well as a strong band to higher energy of the 6a fundamental which we assign here to a mode best described as a hybrid between the 8a and 8b modes. It would be tempting, in the absence of the CASSCF results, to associate the 8a/8b band with the second of the two bands appearing around 620 cm<sup>-1</sup> in the experimental spectrum. However, such an assignment would conflict with the established assignment of this pair of bands in pyrimidine to the 6a<sup>1</sup>/6b<sup>2</sup> Fermi resonance. Moreover, no such activity is seen in any of the CASSCF simulations and as a result we are inclined to conclude that in this case, the CASSCF simulations provide the

most consistent and straightforward match to experiment in line with the expected strengths of a multi-reference method such as CASSCF in producing more accurate excited state geometries than typically is the case with single-reference CC2. Notwithstanding the relatively small detail differences between simulations deriving from different computational methods, the generally good match between simulations and experiment provide additional supporting evidence to the case that the R2PI spectrum derives wholly from the  $\sigma_B$ -conformer.

On this basis, we can use the Franck-Condon simulations presented in Figure 6 to facilitate a vibrational assignment of some of the lower wavenumber intermolecular bands as well as the bands appearing to higher internal energy in the spectrum. Five bands appear most prominently below 300 cm<sup>-1</sup> and of these, the first at 44.7 cm<sup>-1</sup> is assigned with a reasonably high degree of confidence to the fundamental in the in-plane bend,  $\beta'$ , based on the fact that it is the lowest wavenumber in-plane van der Waals mode and is therefore more likely to be excited in single quanta than out-of-plane modes whose dipoles are oriented perpendicular to the transition dipole moment. The next band at 79.1 cm<sup>-1</sup> could be assigned with reasonable conviction either to the van der Waals stretch fundamental,  $\sigma$ , or conceivably to the out-of-plane rock,  $\rho''$ , but again, the latter might not be expected to appear with an intensity which competes with the in-plane stretch because it is polarised normal to the transition dipole moment. We are inclined therefore to err on the conservative side and assign this band to the van der Waals stretch. The strongest of the van der Waals bands appears at 128.2 cm<sup>-1</sup> with assignment to either the first overtone in the out-of-plane rock, or to a transition involving the ammonia internal rotation,  $\tau$ , being the most plausible. The assignment of the band at 242.1 cm<sup>-1</sup> is rather more straightforwardly made to the fundamental in the in-plane rock,  $\rho'$ . With the bands at 325.6, 604.1 and 655.7 cm<sup>-1</sup> already assigned to the 6b<sup>1</sup>, 6a<sup>1</sup> and 6b<sup>2</sup> vibrations, the weaker features at 680.2, 732.7 and 782.1 cm<sup>-1</sup> naturally assign as combination bands involving 6a<sup>1</sup> and 6b<sup>2</sup> with the van der Waals stretch and out-of-plane rock/internal rotation (see Table 1 for complete assignment).

## 5. Conclusions

The experimental and computational results reported in the present work provide compelling evidence that pyrimidine...NH<sub>3</sub> favours a single stable conformation in which the ammonia binds *via* two hydrogen bonds within the plane of the ring, in a location which minimises repulsion between the ammonia nitrogen lone pair and that of the second pyrimidine nitrogen in the 3 position on the opposite side of the ring. None of the evidence obtained as part of this work supports the conclusion of previous work that the complex adopts a  $\pi$ -bound structure in which the ammonia sits above the aromatic ring.

Geometry optimisations conducted at the RICC2, MP2 and CASSCF levels of theory identified three stable Pyr-NH<sub>3</sub> conformations in the  $S_0$  state, two of which, named  $\sigma_A$  and  $\sigma_B$ ,

feature double hydrogen-bound pseudo five-membered rings in which, for the former, the ammonia bridges the nitrogen in the 1 position and the carbon in the 2 position whilst in the latter, the ammonia bridges the carbon in the 6 position with the nitrogen in the 1 position. The third conformation is one in which the ammonia sits above the ring, forming a pair of hydrogen bonds between two of the ammonia hydrogens and the two ring nitrogens, and with the electron-deficient  $\pi$ -system accepting partial charge from the ammonia lone pair. Of these three conformations, the  $\sigma_B$ -conformer is comfortably the most stable, as determined from computed CCSD(T)/CBS interaction energies, and the  $\pi$ -conformation the least. The greater stability of the  $\sigma_B$ -conformer derives from the much smaller long-range cross-repulsion between the ammonia nitrogen and the pyrimidine ring nitrogen on the opposite side of the ring. The exposure of the ammonia to the more remote nitrogen in the  $\sigma_A$  complex acts to destabilise it by as much as 20% compared with  $\sigma_B$ .

Excited state geometry optimisations conducted at the RICC2 and CASSCF levels of theory failed to yield a stable  $\pi$ -bound structure for the  $S_1$  ( $\pi^*(a_2) \leftarrow n_N(b_2)$ ) state but optimisations conducted for the two in-plane  $\sigma$ -structures converged to stable minima following relatively modest changes in binding geometry of the ammonia. All excited state optimisations also revealed that the pyrimidine ring undergoes a ring distortion in which one of the two ring nitrogens moves inboard, breaking the mirror symmetry which exists in the electronic ground state. This distortion arises as a consequence of the  $\pi^* \leftarrow n$  excitation which results in seven  $\pi$ -electrons and an anti-aromatic ring. The resulting distortion of the ring leads to uneven bond angles about the two ring nitrogens with electron density favouring the nitrogen with the smaller bond angle and it is to this side of the ring that the ammonia binds in both  $\sigma_A$  and  $\sigma_B$  conformers. For the  $\sigma_B$  conformer, in which the ammonia is located in a position more remote from the second ring nitrogen, electronic excitation weakens the interaction as the lone-pair electron density reduces on the ring nitrogen involved in the cyclic hydrogen bonded structure. However, for the  $\sigma_A$  conformer in which the ammonia lone pair is exposed to the second ring nitrogen, the reduction in cross-repulsion that results from electronic excitation outweighs the weakening of the direct hydrogen bond to the  $N_1$  nitrogen with the result that the interaction strengthens in the excited state. The result is a substantial predicted red-shift for the  $\sigma_A$ -conformer and an even larger predicted blue-shift for the  $\sigma_B$ -conformer. The experimental observation of a blue-shift of  $+369 \text{ cm}^{-1}$  in the R2PI spectrum of  $\text{Pyr} \cdots \text{NH}_3$  taken together with the fact that the  $\sigma_B$ -conformer has comfortably the largest computed ground state interaction energy leads to a confident assignment of the R2PI spectrum as deriving wholly from the  $\sigma_B$ -conformer. Multidimensional Franck-Condon simulations based on the computed ground and excited state structures yielded simulations which compared well with experiment and provided a means to make reasonably confident vibrational assignments of the R2PI spectrum.

It seems clear from the results presented here that the presence of two ring nitrogens in a hetero-aromatic molecule such as pyrimidine renders the ring so  $\pi$ -electron deficient that formation of stable  $\pi$ -hydrogen bonds with proton donors is highly unlikely. Furthermore, although the  $\pi$ -system may alternatively offer a means to bind an electron-donating solvent in an above-ring conformation, the much stronger attraction of the lone-pairs on the ring makes in-plane double hydrogen-bonded conformations far more viable.

## Acknowledgements

The EPSRC National Service for Computational Chemistry Software is gratefully acknowledged for computing time and access to Turbomole and Gaussian. URL: <http://www.nscs.ac.uk>.

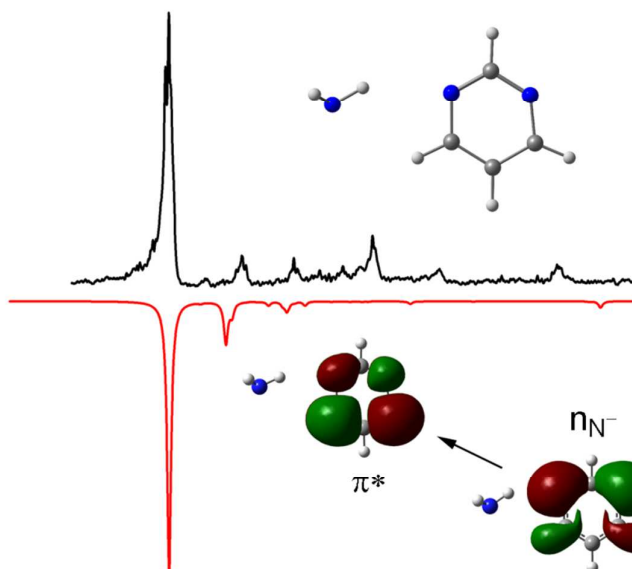
## Notes and references

<sup>a</sup> Department of Chemistry, University of York, Heslington, York YO10 5DD, UK. Fax: +44 1904 322516; Tel: +44 1904 324534; E-mail: [martin.cockett@york.ac.uk](mailto:martin.cockett@york.ac.uk)

Electronic Supplementary Information (ESI) available: Cartesian coordinates for optimised ground and excited state structures of the complex are given in the Supplementary information. See DOI: 10.1039/b000000x/

- 1 R. Wintjens, J. Liévin, M. Rooman, E. Buisine, *J. Mol. Biol.*, 2000, **302**, 395.
- 2 M. Rooman, J. Liévin, E. Buisine and R. Wintjens, *J. Mol. Biol.* 2002, **319**, 67.
- 3 R. Hochstrasser and C.J Marzocco, *J. Mol. Spectrosc.*, 1972, **42**, 75.
- 4 A.E.W. Knight, C.M. Lawburgh and C.S. Parmenter, *J. Chem. Phys.* 1975, **63**, 4336.
- 5 K.K. Innes, I.G. Ross and W.R. Moomaw, *J. Mol. Spectrosc.* 1988, **132**, 492.
- 6 M. Riese and J. Grotemeyer, *Anal Bioanal Chem*, 2006, **386**, 59.
- 7 I. Yamazaki, T. Murao, T. Yamanaka and K. Yoshihari, *Faraday Discuss. Chem. Soc.*, 1983, **75**, 395.
- 8 U. Lottermoser P. Rademacher, M. Mazik, and K. Kowski, *Eur. J. Org. Chem*, 2005, 522.
- 9 J. E. Del Bene, J. D. Watts and R. J. Bartlett, *J. Chem. Phys.* 1997, **106**, 6051.
- 10 G. Fischer, Z. Cai, J. R. Reimers and P. Wormell, *J. Chem Phys.* 2003, **107**, 3093.

- 
- 
- 11 S. Sato, K. I. Omiya and K. Kimura, *Journal of Electron Spectroscopy and Related Phenomena*, 1998, **97**, 121.
  - 12 G. Maes, J. Smets, L. Adamowics, W. McCarthy, M. K. Van Bael, L. Houben and K. Schoone, *J. Mol. Struct.*, 1997, **315**, 410.
  - 13 S. Schlucker, J. Koster, R. K. Singh and B. P. Asthana, *J. Phys. Chem. A.*, 2007, **111**, 5185.
  - 14 J. C. Howard, N. I. Hammer and G. S. Tschumper, *Chem. Phys. Chem. Special Issue: Computational Chemistry.*, 2011, **12**(17), 3262.
  - 15 Z.-L. Cai and J. R. Reimers, *J. Chem. Phys. Chem. A.*, 2005, **109**, 1576.
  - 16 J. Wanna, J. A. Menapace and E. R. Bernstein, *J. Chem. Phys.*, 1986, **85**(4), 1795.
  - 17 J. Zeng, N. S. Hush and J. R. Reimers, *J. Chem. Phys.*, 1993, **99**(3), 1496.
  - 18 N.M. Tonge, E.C. MacMahon, I. Pugliesi and M.C.R. Cockett, *J. Chem. Phys.* 2007, **126**, 154319.
  - 19 M. P. Gosling, I. Pugliesi and M. C. R. Cockett., *Phys. Chem. Chem. Phys.*, 2010, **12**, 132.
  - 20 M.J. Watkins, M.C.R. Cockett, *J. Chem. Phys.* **2000**, **113**, 10560.
  - 21 M.J. Frisch, *et al.* Gaussian, Inc., Wallingford CT, (2009).
  - 22 R. Ahlrichs, M. Bär, M. Häser, H. Horn and C. Kölmel, *Chem. Phys. Lett.* 1989, **162**, 165.
  - 23 C. Møller and M.S. Plesset, *Phys. Rev.* 1934, **46**, 618.
  - 24 K. Shibasaki, A. Fujii, N. Mikami and S. Tsuzuki, *J. Phys. Chem. A*, 2007, **111**, 753.
  - 25 T. Helgaker, W. Klopper, H. Koch and J. Noga, *J. Chem. Phys.* 1997, **106**, 9639
  - 26 J. Šponer, K.E. Riley and P. Hobza, *Phys. Chem. Chem. Phys.* 2008, **10**, 2595.
  - 27 P. Hobza and J. Šponer, *Chem. Rev.* 1999, **99**, 3247.
  - 28 J. Řezáč, K.E. Riley and P. Hobza, *J. Chem. Theory Comput.* 2011, **7**, 2427.
  - 29 J. Řezáč, K.E. Riley and P. Hobza, *J. Chem. Theory Comput.* 2011 **7**, 3466.
  - 30 O. Christiansen, H. Koch and P. Jørgensen, *Chem. Phys. Lett.* 1995, 243, 409.
  - 31 C. Hättig and F. Weigend, *J. Chem. Phys.* 2000, **113**, 5154.
  - 32 A. Schäfer, C. Huber and R. Ahlrichs, *J. Chem. Phys.* 1994, **100**, 5829.
  - 33 F. Weigand, F. Furche and R. Ahlrichs, *J. Chem. Phys.* 2003, **119**, 12753.
  - 34 I. Pugliesi and K. Müller-Dethlefs, *J. Phys. Chem. A*, 2006, **110**, 4657.
  - 35 M. Riese, Z. Altug and J. Grotemeyer, *Phys. Chem. Chem. Phys.*, 2006, **8**, 4441.
  - 36 K-W. Choi, D-S. Ahn, S. Lee, H. Choi, K-K. Baeck, S-U. Heo, S. J. Baek, Y. S. Choi and S. K. Kim, *Chem. Phys. Chem.*, 2004, **5**, 737.
  - 37 E.V. Doktorov, I.A. Malkin and V.I. Man'ke, *J. Mol. Spectrosc.* 1977, **64**, 302.
  - 38 F. Duschinsky, *Acta Physicochim. URSS*, 1937, **7**, 551.
  - 39 J.T. Hougen and J.K.G Watson, *Can. J. Phys.* 1965, **43**, 298.
  - 40 All Franck-Condon simulations have been carried out using FC-Lab2 Version 2009.a, a computational package developed by C. Schrieffer, M.C.R. Cockett and I. Pugliesi. The latest information on program updates, a basic introduction to Franck-Condon simulations and a free download of the software can be found at <http://www.fclab2.net/>.



The pyrimidine...NH<sub>3</sub> complex exists as just a single double hydrogen-bonded structure in the gas phase with the ammonia favouring a position which shields it from repulsive interactions with the more remote ring-nitrogen.